

Air Force Institute of Technology

AFIT Scholar

Faculty Publications

10-27-2008

Controlling the Transmitted Field into a Cylindrical Cloak's Hidden Region

Jeffrey S. McGuirk

Peter J. Collins

Air Force Institute of Technology

Follow this and additional works at: <https://scholar.afit.edu/facpub>



Part of the [Optics Commons](#)

Recommended Citation

McGuirk, J. S., & Collins, P. J. (2008). Controlling the transmitted field into a cylindrical cloak's hidden region. *Optics Express*, 16(22), 17560. <https://doi.org/10.1364/OE.16.017560>

This Article is brought to you for free and open access by AFIT Scholar. It has been accepted for inclusion in Faculty Publications by an authorized administrator of AFIT Scholar. For more information, please contact richard.mansfield@afit.edu.

Controlling the transmitted field into a cylindrical cloak's hidden region

Jeffrey S. McGuirk* and Peter J. Collins

*Air Force Institute of Technology
Department of Electrical and Computer Engineering
2950 Hobson Way
Wright Patterson AFB, OH 45433
jeffrey.mcguirk@afit.edu*

Abstract: Constitutive parameters for simplified cylindrical cloaks have been developed such that $\epsilon_z\mu_\theta$ and $\epsilon_z\mu_r$ match those of the ideal cylindrical cloak. Although they are not perfect, simplified cylindrical cloaks have been shown to inherit many of the power-bending properties of the ideal cloak. However, energy is transmitted into simplified cloaks' hidden regions. Here, we develop a constraint equation that can be used to determine how closely field behavior within the simplified cylindrical cloak matches that of the ideal cloak. The deviation from this controlling equation can be reduced by controlling the cloak's parameter value, μ_θ . As the deviation from our constraint equation is decreased, the field transmitted into the cloak's hidden region is reduced, resulting in less energy impinging on the cloaked object. This results in a smaller scattered field due to the presence of the cloaked object. However, the resulting impedance mismatch at $r = b$ results in a significant scattered field by the cloak itself. Thus, we have found when using cylindrical cloaks that satisfy the ideal values of $\epsilon_z\mu_\theta$ and $\epsilon_z\mu_r$ for scattering width reduction, it is more important to have a matched impedance at $r = b$ than to have a smaller field transmitted into the cloak's hidden region. However, such cloaks' scattering widths can vary significantly as a function of the object in the hidden region. A cloak with a matched impedance at $r = b$ and that satisfies specific values for $\epsilon_z\mu_\theta$ and μ'_θ performs reasonably well in terms of scattering width reduction in certain angular regions while being independent of the object in the hidden region.

© 2008 Optical Society of America

OCIS codes: (230.3205) Invisibility cloaks (290.5839) Scattering, invisibility; (260.0260) Physical Optics; (260.2110) Electromagnetic Optics (160.3918) Metamaterials

References and links

1. A. Alù and N. Engheta, "Achieving transparency with plasmonic and metamaterial coatings," *Phys. Rev. E* **72**, 016623 (2005).
2. A. Alù and N. Engheta, "Plasmonic materials in transparency and cloaking problems: mechanism, robustness, and physical insights," *Opt. Express* **15**, 6, 3318-3332 (2007).
3. M. G. Silveirinha, A. Alù and N. Engheta, "Parallel-plate metamaterials for cloaking structures," *Phys. Rev. E* **75**, 036603 (2007).
4. U. Leonhardt, "Optical conformal mapping," *Science* **312**, 1777-1780 (2006).
5. J. B. Pendry, D. Schurig, and D. R. Smith, "Controlling electromagnetic fields," *Science* **312**, 1780-1782 (2006).
6. S. A. Cummer, B. I. Popa, D. Schurig, D. R. Smith, and J. Pendry, "Full-wave simulations of electromagnetic cloaking structures," *Phys. Rev. E* **74**, 036621 (2006).

7. H. Ma, S. Qu, Z. Xu, J. Zhang, B. Chen, and J. Wang, "Material parameter equation for elliptical cylindrical cloaks," *Phys. Rev. A* **77**, 013825 (2008).
 8. D. Kwon and D. Werner, "Two-dimensional eccentric elliptic electromagnetic cloaks," *Appl. Phys. Lett.* **92**, 013505 (2008).
 9. M. Rahm, D. Schurig, D. A. Roberts, S. A. Cummer, D. R. Smith, and J. B. Pendry, "Design of electromagnetic cloaks and concentrators using form-invariant coordinate transformations of Maxwell's equations," *Photon. Nanostruct.: Fundam. Appl.* **6**, 87 (2008).
 10. D. Schurig, J. B. Pendry, and D. R. Smith, "Calculation of material properties and ray tracing in transformation media," *Opt. Express* **14**, 21, 9794-9804 (2006).
 11. Z. Ruan, M. Yan, C. W. Neff, and M. Qiu, "Ideal cylindrical cloak: Perfect but sensitive to tiny perturbations," *Phys. Rev. Lett.* **99**, 113903 (2007).
 12. H. Chen, B. I. W. B. Zhang, and J. A. Kong, "Electromagnetic wave interactions with a metamaterial cloak," *Phys. Rev. Lett.* **99**, 063903 (2007).
 13. G. Isić, R. Gajić, B. Novaković, Z. V. Popović, and K. Hingerl, "Radiation and scattering from imperfect cylindrical electromagnetic cloaks," *Opt. Express* **16**, 1413-1422 (2008).
 14. D. Schurig, J. J. Mock, B. J. Justice, S. A. Cummer, J. B. Pendry, A. F. Starr, and D. R. Smith, "Metamaterial electromagnetic cloak at microwave frequencies," *Science* **314**, 977-980 (2006).
 15. M. Yan, Z. Ruan, and M. Qiu, "Cylindrical invisibility cloak with simplified material parameters is inherently visible," *Phys. Rev. Lett.* **99**, 233901 (2007).
 16. W. Cai, U. K. Chettiar, A. V. Kildishev, and V. M. Shalaev, "Optical cloaking with metamaterials," *Nat. Photonics* **1**, 224-227 (2007).
 17. W. Cai, U. K. Chettiar, A. V. Kildishev, V. M. Shalaev, and G. W. Milton, "Nonmagnetic cloak with minimized scattering," *Appl. Phys. Lett.* **91**, 111107 (2007).
 18. M. Yan, Z. Ruan, and M. Qiu, "Scattering characteristics of simplified cylindrical invisibility cloaks," *Opt. Express* **15**, 26, 17772-17782 (2007).
-

1. Introduction

The ability to make objects invisible to all types of electromagnetic radiation has received considerable attention in recent years. It has been shown it is possible to reduce the scattering width of objects using lossless plasmonic or metamaterial covers [1-3], although these methods depend on the geometry and the material properties of the target object. An alternative method to reduce or even eliminate the scattering cross section that is independent of the target object involves designing cloaks of any geometry whose constitutive parameters can be derived based on a coordinate transformation [4, 5]. The cloak is a complex anisotropic, spatially varying material that effectively guides electromagnetic waves around the desired hidden region. The fields emerge from the cloak unperturbed as they would if they were propagating in free space. Full-wave two dimensional simulations have been performed on a variety of cloak geometries whose constituent parameters are found using the method developed in [5]. Such geometries include a cylinder [6], an elliptical cylinder [7], an eccentric elliptical cylinder [8], and a square [9]. All results clearly show the cloaked region is effectively hidden from incident electromagnetic radiation while the cloaking structures do not cause scattered electromagnetic fields. Analysis of spherical and cylindrical cloaks using ray tracing showed incident rays were effectively guided around the cloaked region without any perturbation to the field structure outside the cloaking body [10]. Analysis using boundary conditions to determine the scattering and transmission coefficients at the boundaries of a cylindrical cloak concluded the cylindrical cloak with the ideal constitutive parameters renders a region invisible to incident fields while exciting no scattered field [11]. A full wave Mie scattering model was used to analyze the interactions of electromagnetic waves with a spherical cloak [12]. Like the cylindrical cloak, the spherical cloak, whose material properties are derived in the same fashion, was found to perfectly cloak a given region of space with no resulting scattered field. Therefore, there is agreement amongst the community that ideal cloaks whose constitutive parameters are derived using the approach shown in [5] result in a region that is completely shielded from electromagnetic radiation while not inducing any type of scattered field. Hence, an object placed within the hidden region is effectively cloaked.

There has been considerable analysis of cylindrical cloaks. The constitutive parameters for the ideal cylindrical cloak found using the method described in [5] are shown in Eq. (1).

$$\epsilon_r = \mu_r = \frac{r-a}{r}, \quad \epsilon_\theta = \mu_\theta = \frac{r}{r-a}, \quad \epsilon_z = \mu_z = \frac{r-a}{r} \left(\frac{b}{b-a} \right)^2 \quad (1)$$

Note a and b are the radii of the inner and outer cloak boundaries respectively as shown in Fig. 1. For this work, all simulations used settings such that $a = \lambda$ and $b = 2\lambda$ where λ is

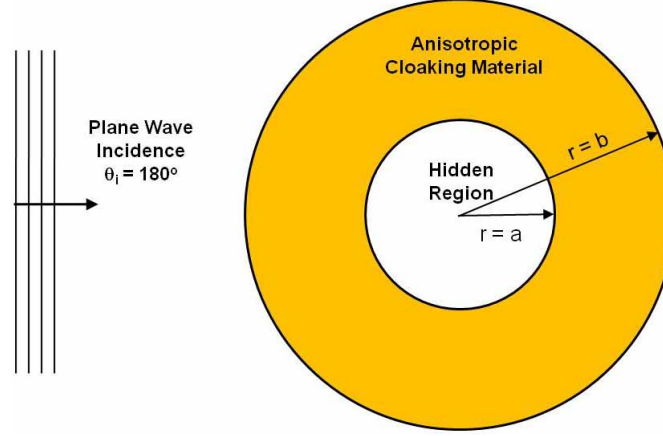


Fig. 1. Cylindrical cloak geometry. For this effort, $a = \lambda$ and $b = 2\lambda$. Additionally, plane wave incidence is assumed throughout with the wave travelling in the \hat{x} direction (i.e. $\theta_i = 180^\circ$).

the wavelength of the incident radiation. Plane wave incidence is assumed with the plane wave travelling in the \hat{x} direction.

Materials with the properties shown in Eq. (1) are not naturally occurring. However, recent advances in metamaterials show promise in approaching the constitutive parameters required for cloaking. Metamaterials are materials with subwavelength microstructures that are designed to have desired electric and magnetic properties. Despite the latest advances in metamaterials, we do not currently have the ability to manufacture a cylindrical cloak with the ideal constitutive parameters. This is because all of the ideal constitutive parameters are anisotropic and spatially varying, and it is not yet possible to realize such a material. However, by assuming either a transverse magnetic (TM) or transverse electric (TE) incident field, the required constitutive parameter set is simplified from six to three relevant parameters. This does not yet solve the issues of spatial variance or anisotropy, but it will lead to further parameter simplifications, which will be discussed below.

For this work, we will assume TM^z incident fields (the electric field is purely \hat{z} directed). Thus, only ϵ_z , μ_r , and μ_θ are required when analyzing the field behavior. We can use the relevant parameters along with Maxwell's equations to define a wave equation that governs the field behavior within the ideal cylindrical cloak (the region $a < r < b$).

Maxwell's equations for an assumed TM^z incident field can be used to find the relationship between the field components. These are shown in Eqs. (2), (3), and (4).

$$H_r = -\frac{1}{j\omega\mu_r r} \frac{\partial E_z}{\partial \theta} \quad (2)$$

$$H_\theta = \frac{1}{j\omega\mu_\theta} \frac{\partial E_z}{\partial r} \quad (3)$$

$$E_z = \frac{1}{j\omega\epsilon_z r} \left[\frac{\partial(rH_\theta)}{\partial r} - \frac{\partial H_r}{\partial \theta} \right] \quad (4)$$

Equations (2) and (3) can be used in Eq. (4) to develop a general wave equation governing the behavior of TM^z fields within a complex anisotropic material with spatially varying constitutive parameters ϵ_z , μ_r , and μ_θ .

$$\frac{1}{\epsilon_z r} \left[\frac{\partial}{\partial r} \left(\frac{r}{\mu_\theta} \frac{\partial E_z}{\partial r} \right) \right] + \frac{1}{\epsilon_z r^2} \frac{\partial}{\partial \theta} \left(\frac{1}{\mu_r} \frac{\partial E_z}{\partial \theta} \right) + k_o^2 E_z = 0 \quad (5)$$

If we assume all constitutive parameters are θ -invariant but not necessarily r -invariant, the general wave equation can be expanded analytically to

$$\frac{1}{\epsilon_z \mu_\theta} \frac{\partial^2 E_z}{\partial r^2} + \left[\frac{1}{\epsilon_z \mu_\theta} \frac{1}{r} - \frac{\mu'_\theta}{\epsilon_z \mu_\theta^2} \right] \frac{\partial E_z}{\partial r} + \frac{1}{\epsilon_z \mu_r} \frac{1}{r^2} \frac{\partial^2 E_z}{\partial \theta^2} + k_o^2 E_z = 0 \quad (6)$$

Note ' implies differentiation with respect to r . When one uses the ideal cylindrical cloak's material parameters shown in Eq. (1) in the general wave equation shown in Eq. (6), the result is the wave equation for TM^z fields in an ideal cylindrical cloak. This is shown in Eq. (7).

$$\left(\frac{b-a}{b} \right)^2 \frac{\partial^2 E_z}{\partial r^2} + \left(\frac{b-a}{b} \right)^2 \frac{1}{r-a} \frac{\partial E_z}{\partial r} + \left(\frac{b-a}{b} \right)^2 \left(\frac{1}{r-a} \right)^2 \frac{\partial^2 E_z}{\partial \theta^2} + k_o^2 E_z = 0 \quad (7)$$

Theoretically, cloaks constructed with the ideal material parameters will perfectly hide any object placed in the hidden region. For TM^z fields, at $r = a$ the required material parameters are $\mu_r = 0$, $\epsilon_z = 0$, and $\mu_\theta = \infty$. Such values are not achievable even in metamaterials. Therefore, the impact of manufacturability on cloak performance has been analyzed. It has been shown there is significant reduction in cloak scattering width performance when even the slightest deviation in μ_r is introduced [11, 13]. Though this degradation in cloak performance exists, cloaking is still an interesting and viable option for both signature reduction and for shielding objects from incident radiation. In order to create a manufacturable cloak, simplifications to the ideal material parameters must be made. An initial set of simplified parameters was developed in [14]. These are shown in Eq. (8). Note only one parameter, μ_r is spatially varying, significantly improving the cloak's manufacturability.

$$\mu_r = \left(\frac{r-a}{r} \right)^2, \quad \mu_\theta = 1, \quad \epsilon_z = \left(\frac{b}{b-a} \right)^2 \quad (8)$$

The material parameters shown in Eq. (8) were initially thought to satisfy the same wave equation as the ideal parameter set. However, Yan *et al.* state the procedure leading to this conclusion was questionable, and they clearly show the simplified and ideal parameter sets satisfy different wave equations [15]. This is explicitly seen by substituting the simplified cloak's material parameters into Eq. (6) which results in the wave equation shown in Eq. (9).

$$\left(\frac{b-a}{b} \right)^2 \frac{\partial^2 E_z}{\partial r^2} + \left(\frac{b-a}{b} \right)^2 \frac{1}{r} \frac{\partial E_z}{\partial r} + \left(\frac{b-a}{b} \right)^2 \left(\frac{1}{r-a} \right)^2 \frac{\partial^2 E_z}{\partial \theta^2} + k_o^2 E_z = 0 \quad (9)$$

Note the subtle difference in Eq. (9) compared to Eq. (7). The wave equation resulting from the simplified parameters has a $1/r$ factor in front of the $\partial E_z / \partial r$ term. The wave equation resulting from the ideal parameters has a factor of $1/(r-a)$ for this same term. Thus, for values such that $r \gg a$, the field behavior of the two cloaks will be similar [15], but they certainly do not satisfy the same wave equation. Since the ideal cylindrical cloak effectively guides electromagnetic

energy around the region, $r < a$, it makes sense that a simplified cloak, whose wave equation differs from that of the ideal cloak, has energy transmitted into this same region. Yan *et al.* show this transmitted energy is dominated by the zeroth-order field component when an incident plane wave is expressed in terms of cylindrical wave functions [15].

We would like to minimize the energy transmitted into the hidden region. The less energy that is transmitted into this region results in less energy that is scattered by the cloaked object, possibly resulting in a smaller scattered field. In this analysis, we develop the constraints on the cylindrical cloak's constitutive parameters that determine the amount of energy that is transmitted into the cloak's hidden region. We then analyze the cloak's effectiveness in terms of the amount of energy in the hidden region and of the overall scattering width of the cloaking structure.

2. Analysis

By comparing Eqs. (6) and (7), we find the cylindrical cloak's constitutive parameters must meet the following conditions in order to achieve perfect cloaking when a TM^z field is incident.

$$\frac{1}{\varepsilon_z \mu_\theta} = \left(\frac{b-a}{b} \right)^2 \quad (10)$$

$$\frac{1}{\varepsilon_z \mu_r} = \left(\frac{b-a}{b} \right)^2 \left(\frac{r}{r-a} \right)^2 \quad (11)$$

$$\frac{1}{\varepsilon_z \mu_\theta} \frac{1}{r} - \frac{\mu'_\theta}{\varepsilon_z \mu_\theta^2} = \frac{1}{r-a} \left(\frac{b-a}{b} \right)^2 \quad (12)$$

This third constraint equation shown in Eq. (12) has not appeared in the literature and forms the basis for the alternative simplified parameters we propose later in this paper.

The ideal cylindrical cloak also has an impedance at the outer boundary, $r = b$, that matches free space.

$$Z_{ideal} = \sqrt{\frac{\mu_\theta}{\varepsilon_z}} \Big|_{r=b} = 1 \quad (13)$$

There is no reflection at the free space-cloak interface; hence, the cloak is acting like a perfectly matched layer.

The simplified parameters shown in Eq. (8) satisfy Eqs. (10) and (11); they do not satisfy Eq. (12). Additionally, the impedance mismatch at $r = b$ for the cylindrical cloak with the same simplified constitutive parameters is

$$Z_{simp} = \sqrt{\frac{\mu_\theta}{\varepsilon_z}} \Big|_{r=b} = 0.5 \quad (14)$$

Obviously, there will be a scattered field from the simplified cylindrical cloak with an object in its hidden region. However, what is the dominant factor in the scattering field, the impedance mismatch at $r = b$, or is it due to the field transmitted into the cloaked region and impinging the hidden object? This question motivated our investigation discussed in the following paragraphs.

We performed simulations using Comsol Multiphysics on a simplified cylindrical cloak with the parameters shown in Eq. (8). First, we simulated the cloaking structure without any object placed in the hidden region. We then placed a PEC cylinder with radius $r = a$ and a square PEC with side length a in the hidden region. These objects were chosen because our intent is to show objects with different scattering properties placed in the hidden region impact the cloak's overall scattered field. Since our simulation wavelength is $\lambda = a$, the objects placed

in the hidden region are on the order of one wavelength in size. In this electrical size regime, scattering is largely due to the volume of the object. Our chosen objects have significantly different volumes; thus, the overall scattered fields should differ due to field penetration into the hidden region. These results are shown in Fig. 2. Note the fields in the hidden region for

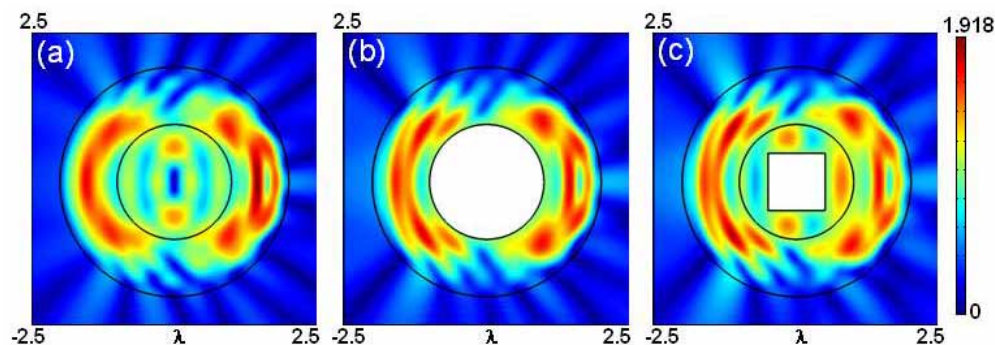


Fig. 2. Scattered electric field magnitude for a simplified cylindrical cloak that has (a) nothing in its hidden region, (b) PEC cylinder with radius a in the hidden region, and (c) square PEC of side length a in the hidden region.

the empty cloak, an expected result based on the work done in [15]. Based on these images, it is difficult to fully comprehend the size and pattern of the scattered field for each geometry. Therefore, we transformed the Comsol simulation results to a far zone two-dimensional radar cross section i.e. scattering width. We determined each geometry's scattering width and plotted the result as a function of θ . This is shown in Fig. 3. Every scattering width plot in this paper is

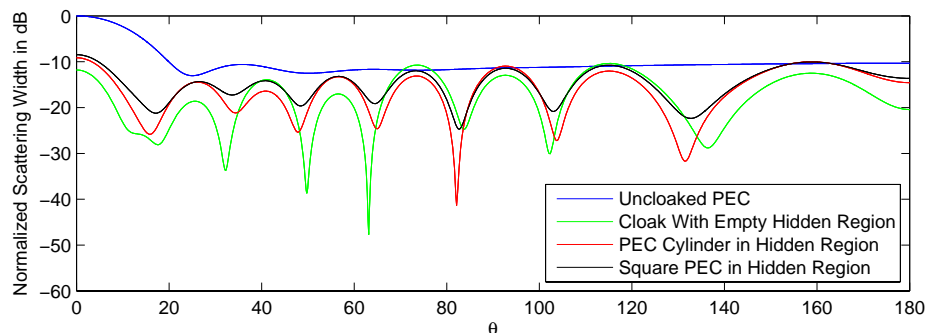


Fig. 3. Scattering from a simplified cloak. The blue line is the scattering width for an uncloaked PEC normalized by its maximum field value, the green line shows the scattering width for an empty simplified cloak normalized by the maximum value for the scattered field from an uncloaked PEC, the red line is the scattering width for a simplified cloak with a PEC cylinder of radius a in the hidden region normalized using the same factor, and the black line is the scattering width for the cloak with a square PEC in the hidden region, also normalized by the same factor.

normalized by the maximum scattering width value for an uncloaked PEC cylinder of radius a .

Note the cloaked PEC cylinder does have a smaller scattering width than an uncloaked PEC cylinder. Also note the variation in the scattering widths. This variation is due to different objects being placed in the hidden region. To better see how the scattering width is changed

when different objects are inserted into the hidden region, we plotted the difference between the scattering width of a cloaked PEC cylinder (the red line in Fig. 3) and the scattering width for a cloaked PEC square (the black line in Fig. 3). The results are shown in Fig. 4. Obviously,

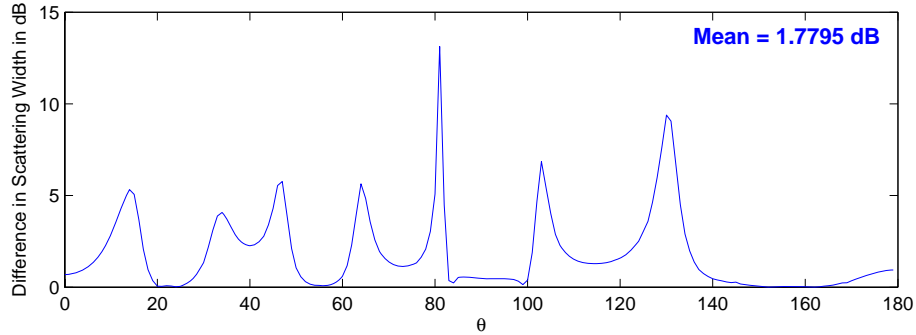


Fig. 4. Scattering width difference for a simplified cloak with a PEC cylinder and a PEC square in the hidden region.

changing the object in the hidden region has an impact on the overall scattered field for this set of constitutive parameters. The question is, will minimizing the field transmitted into the hidden region reduce the overall scattered field variations caused by different objects in the hidden region?

There have been suggested improvements to the original simplified constitutive parameters [16-18]. The improved set of constitutive parameters for TM^z incident fields put forth in [18] are shown in Eq. (15).

$$\mu_r = \left(\frac{r-a}{r}\right)^2 \frac{b}{b-a}, \quad \mu_\theta = \frac{b}{b-a}, \quad \varepsilon_z = \frac{b}{b-a} \quad (15)$$

The improved parameter sets were developed with the goal of reducing the overall scattering width of the cloaking structure by matching the cloak's impedance to free space at $r = b$ while still satisfying the requirements shown in Eqs. (10) and (11). As with the initial simplified parameters, improved sets of constitutive parameters do not satisfy the third constraint equation shown in Eq. (12).

We performed Comsol simulations of a cylindrical cloak with the constitutive parameters shown in Eq. (15). We simulated the cloak with no object in the hidden region, with a PEC cylinder of radius a in the hidden region, and with a square PEC with side length a in the hidden region. The results are shown in Fig. 5. It is obvious the scattered field magnitudes in the region $r > b$ are larger for the two cloaks with objects in the hidden region. To better show this, we again transformed the scattered field results to the far zone. These results are shown in Fig. 6. Note how the scattered field from the empty cloak is greatly reduced when compared to the scattered field from the empty cloak with the original set of simplified parameters (Fig. 3, green line). This is due to the matched impedance at $r = b$. Obviously the goal of reducing the overall scattering width from a cloak with simplified parameters was achieved using the constitutive parameters shown in Eq. (15). However, notice how the scattered fields have a greater change in magnitude when the objects in the hidden region are changed. As before, we can better see this by comparing the difference in the scattering widths for the cloaked PEC cylinder (red line in Fig. 6) and the cloaked square PEC (black line in Fig. 6). This is shown in Fig. 7. Note how the average difference in scattering width for a simplified cylindrical cloak with the parameters shown in Eq. (8) with a cylinder and square in the hidden region is

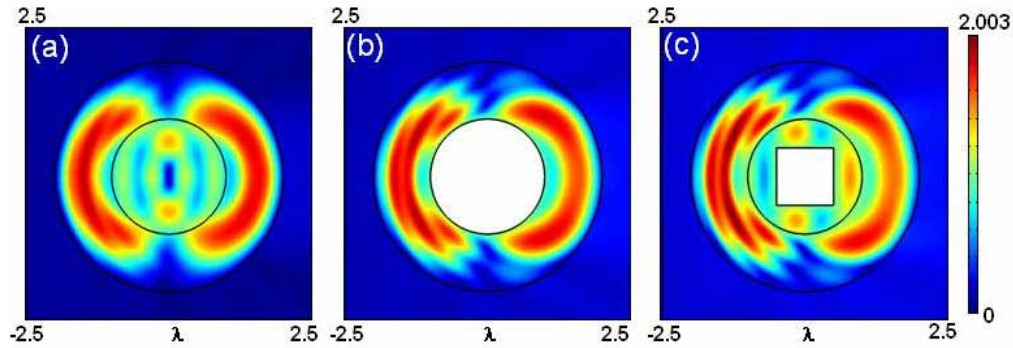


Fig. 5. Scattered electric field magnitude for an improved simplified cylindrical cloak with material parameters put forth [18]. The cloak in image (a) has nothing in its hidden region, image (b) results are for a cloak with a PEC cylinder of radius a in the hidden region, and image (c) results are for a cloak with a square PEC of side length a in the hidden region.

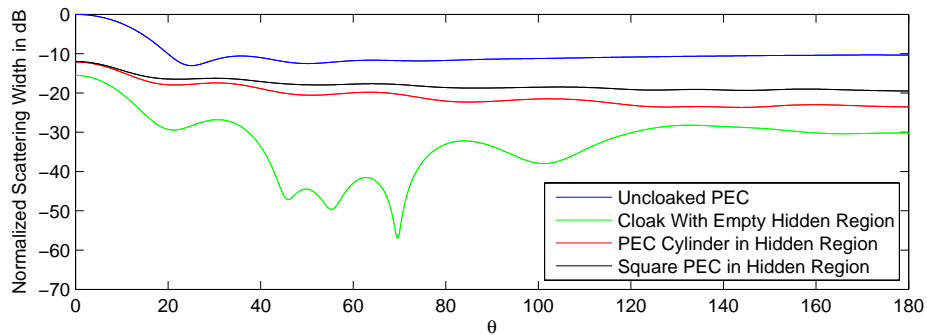


Fig. 6. Normalized scattering widths from an improved simplified cloak. The blue line is the normalized scattering width for an uncloaked PEC, the green line shows the normalized scattering width for an empty simplified cloak with the improved constitutive parameter set, the red line is normalized scattering width for the same cloak but with with a PEC cylinder of radius a in the hidden region, and the black line is the normalized scattering width for the cloak with a square PEC in the hidden region.

1.77 dB. The average difference in scattering width for the improved cylindrical cloak with the parameters shown in Eq. (15) is 2.90 dB. Therefore, even though overall scattering width has been reduced (due to the matched impedance at $r = b$), the variation in the scattered fields when different objects are placed in the hidden region suggests more energy is being transmitted into the hidden region of the cloak with the improved constitutive parameters (Eq. (15)) than the hidden region for the cloak with the original simplified parameters (Eq. (8)). Thus, it seems to imply a matched impedance at $r = b$ is more important for signature width reduction to match impedances at $r = b$ than to minimize the field transmitted into the hidden region. We further test this in the next section and show for these two cloaks, it is the value of μ_θ that determines the size of the field transmitted into the hidden region.

3. Reducing field transmission into the hidden region

As previously mentioned, the constitutive parameters of an ideal cloak for TM^z incident waves must satisfy the constraints shown in Eqs. (10), (11), and (12). The simplified cloaks in the

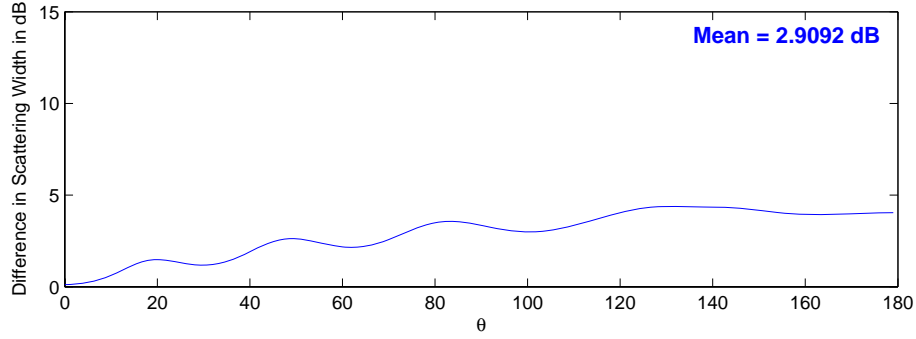


Fig. 7. Scattering width difference for an improved simplified cloak with a PEC cylinder and a square PEC in the hidden region.

literature focus on satisfying Eqs. (10) and (11). Equation (12) has never before been discussed, likely due to the assumptions used when the initial set of simplified parameters was put forth. In what follows, we analyze the importance of Eq. (12) in terms of overall scattering width and of how well the hidden region is shielded from incident energy.

If we first assume a cloak's constitutive parameters satisfy Eqs. (10) and (11), Eq. (12) can be written in a more compact form. This is shown in Eq. (16).

$$\mu'_\theta + \mu_\theta \frac{a}{r(r-a)} = 0 \quad (16)$$

We will initially confine our analysis to cloaks with a constant value for μ_θ (i.e. $\mu'_\theta = 0$). This means the smaller μ_θ , the less error there will be for any value of r when trying to satisfy Eq. (16). We can calculate the left-hand side of Eq. (16) using the simplified values for μ_θ for the initial simplified parameter set and the improved simplified parameter set and plot as a function of r . This is shown in Fig. 8. Two additional plots are shown in this graph, and these will be discussed later. Since the ideal value for Eq. (16) is 0 for all values of r , a larger

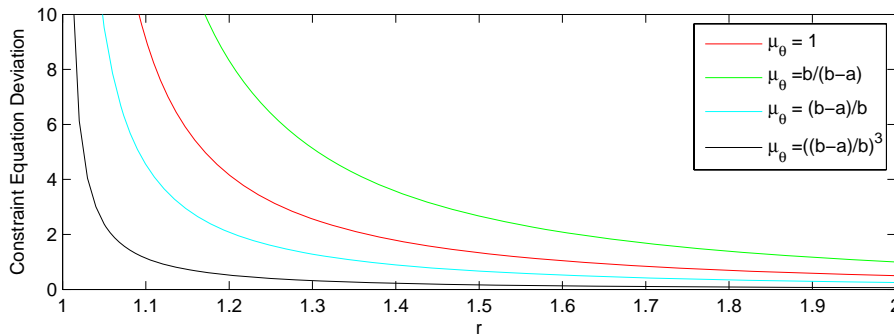


Fig. 8. The calculated values for the left-hand side of Eq. (16) using non-ideal values for μ_θ . The larger the value, the larger the deviation from satisfying the ideal parameter constraint. The red line is for $\mu_\theta = 1$, the green line is for $\mu_\theta = \frac{b}{b-a}$, the cyan line is for $\mu_\theta = \frac{b-a}{b}$, and the black line is for $\mu_\theta = \left(\frac{b-a}{b}\right)^3$.

calculated value for the left-hand side of Eq. (16) using a non-ideal value for μ_θ means a larger

deviation in the material parameter from that of the perfect cloak. This will result in larger fields being transmitted into the hidden region. Based on this graph, we would expect to find the field transmitted into the hidden region for the cloak with the initial simplified parameter set ($\mu_\theta = 1$) to be less than the hidden region field for the improved parameter set ($\mu_\theta = \frac{b-a}{b-a}$). This is due to the fact the value for μ_θ for the initial parameter set results in a smaller error in Eq. (16) than the value for μ_θ in the improved parameter set. Hence, changing objects in the hidden region for the cloak with the original simplified parameters (Fig. 2) would have less impact on the overall scattered field than changing objects in the hidden region of a cloak with the improved parameters (Fig. 5). This is precisely what we have shown in Figs. 4 and 7.

For other parameter sets that satisfy Eqs. (10) and (11) but also minimize the deviation from Eq. (16), the field transmitted into the hidden region should continue to decrease. The parameter sets shown in Eqs. (17) and (18) meet these conditions. The values for μ_θ can be inserted in the left-hand side of Eq. (16), and the results plotted in Fig. 8.

$$\mu_r = \left(\frac{r-a}{r}\right)^2 \frac{b-a}{b}, \quad \mu_\theta = \frac{b-a}{b}, \quad \epsilon_z = \left(\frac{b}{b-a}\right)^3 \quad (17)$$

$$\mu_r = \left(\frac{r-a}{r}\right)^2 \left(\frac{b-a}{b}\right)^3, \quad \mu_\theta = \left(\frac{b-a}{b}\right)^3, \quad \epsilon_z = \left(\frac{b}{b-a}\right)^5 \quad (18)$$

Obviously no attempt was made to match impedances at the $r = b$ interface for the parameter sets shown in Eqs. (17) and (18), as the goal is to show a reduction in the field transmitted into the hidden region. We simulated the cloaks with material parameters shown in Eqs. (17) and (18) with a PEC cylinder of radius a and with a square PEC with side length a in the hidden region. We plotted the difference in the scattering widths for each of these cloaks. The results are shown in Figs. 9 and 10. As expected, the average difference in scattering width

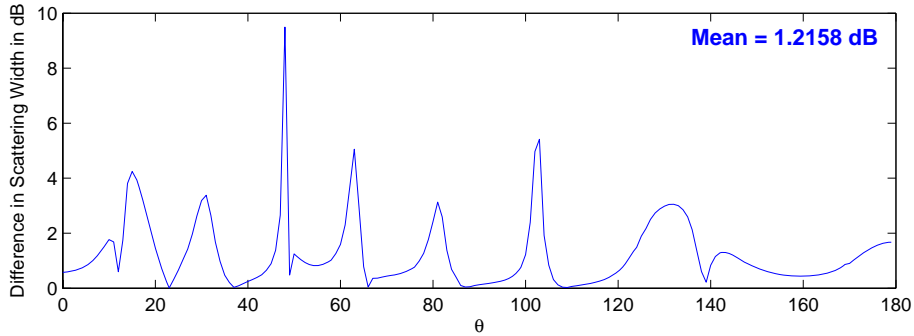


Fig. 9. Scattering width difference for a cloak with parameters shown in Eq. (17) with a PEC cylinder and a square PEC in the hidden region.

is decreased when $\mu_\theta = \frac{b-a}{b}$ and $\mu_\theta = \left(\frac{b-a}{b}\right)^3$ respectively, leading to the conclusion that the field transmitted into the hidden region is being reduced as μ_θ is decreased.

To further show how Eq. (16) determines the amount of energy transmitted into a simplified cylindrical cloak's hidden region, we simulated cloaks with the material parameters shown in Eqs. (8), (15), (17), and (18). We placed no objects in their hidden regions and plotted the total electric field magnitudes in the hidden regions for each cloak. This is shown in Fig. 11. The images in Fig. 11 clearly show that as the cloak takes on values of μ_θ which make the left-hand side of Eq. (16) closer to zero, there is less field transmitted into the hidden region.

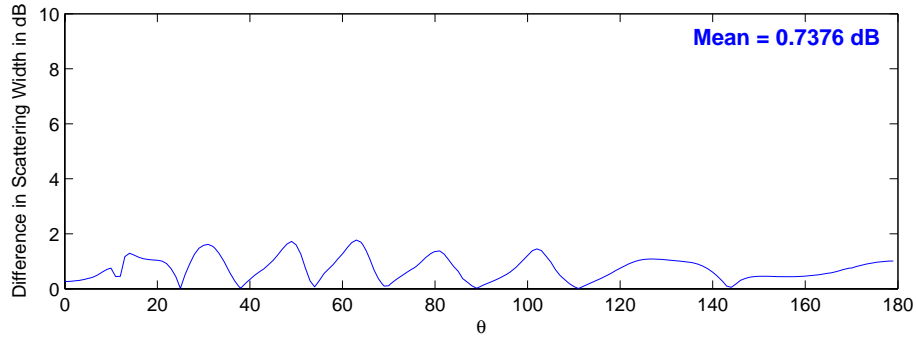


Fig. 10. Scattering width difference for a cloak with parameters shown in Eq. (18) with a PEC cylinder and a square PEC in the hidden region.

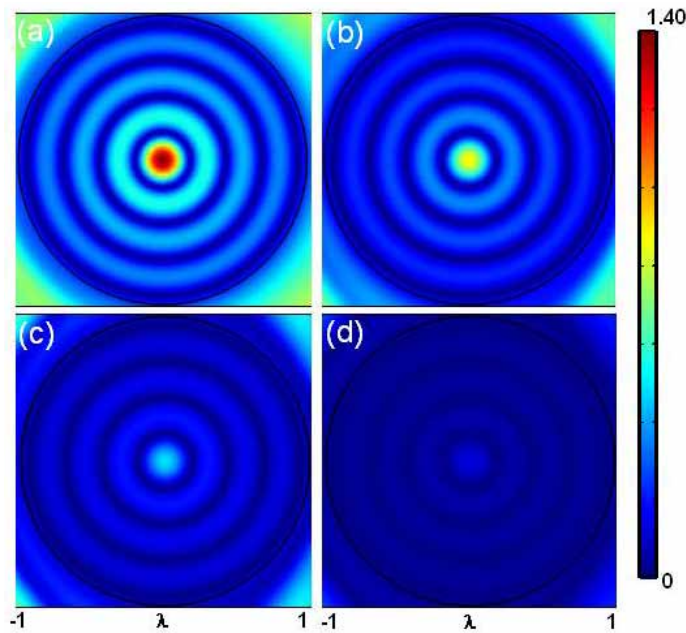


Fig. 11. Electric field magnitude in the hidden region for four different cloaks. Image (a) is for the cloak with material parameters shown in Eq. (15), (b) is for the cloak with material parameters shown in Eq. (8), (c) is for the cloak with material parameters shown in Eq. (17), and (d) is for the cloak with material parameters shown in Eq. (18).

As additional proof, we integrated the energy density at each point in the hidden regions to determine the regions' total energies. These results are shown in Table 1.

Note the cloak with material parameters shown in Eq. (18) has the smallest total energy in the hidden region. Therefore it is the best at shielding the hidden region of the four cloaks considered. However, there is a price to pay for this improved shielding performance. Table 1 also shows the impedance for each cloak at $r = b$. The cloak with the best shielding of the hidden region also has the worst impedance mismatch at the cloak outer boundary. As demonstrated earlier, an impedance mismatch at the boundary results in the cloaking body having a significant scattered field. Therefore, to compare performance in terms of scattering

Table 1. Hidden Region Total Energy and Impedance at $r = b$ for Different Cloaks

μ_θ	Total Energy	$Z _{r=b}$
$\frac{b}{b-a}$	2.76 pJ	1
1	2.24 pJ	0.5
$\frac{b-a}{b}$	1.35 pJ	0.25
$\left(\frac{b}{b-a}\right)^3$	0.42 pJ	0.0625

width, we have plotted the scattering widths for all cloaks with a PEC cylinder of radius a in the hidden region. This is shown in Fig. 12.

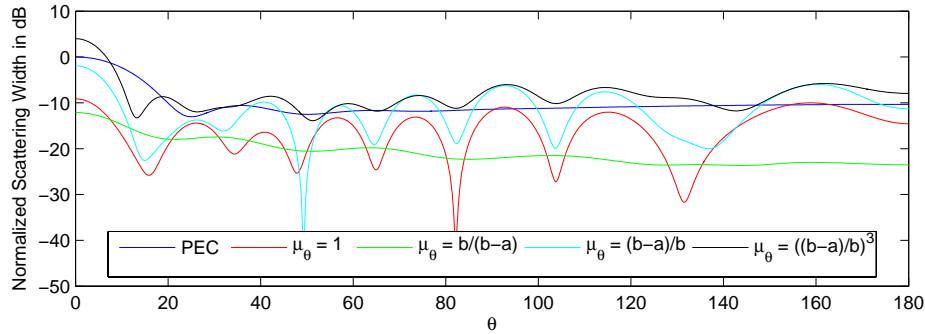


Fig. 12. Scattering widths for cloaks with a PEC cylinder of radius a in the hidden region. The blue line is the normalized scattering width for an uncloaked PEC, the red line is the normalized scattering width for cloak with the simplified parameter set (Eq. (8)), the green line is the scattering width for a cloak with the improved parameter set (15), and the cyan and black lines are the scattering widths for cloaks with parameter sets shown in Eqs. (17) and (18) respectively.

By altering the material parameters such that less fields are transmitted into the hidden region, the change in impedance at $r = b$ dramatically increases the overall scattering width of the cloaking structure. Obviously if scattering width reduction is the goal, use of the improved simplified parameter set (Eq. (15), [18]) is the best option as its scattering width is significantly less than an uncloaked PEC cylinder. Some of the cloaks actually have larger scattering widths at various observation angles than the uncloaked PEC, making them a bad choice if signature reduction is desired. However, if one is attempting to simply shield an object from incident radiation, then the use of Eq. (12) becomes important in that parameters should be chosen such that the deviation from this equation is minimized. One may say shielding can easily be accomplished using a PEC; why use a modified cloak for such a task? A PEC does act as a suitable barrier for a large bandwidth of electromagnetic radiation. However, at extremely low frequencies, skin depths must be considered. It might be less costly, in terms of weight or size, to use a designed cloak for such a shielding application.

We have seen that, in terms of overall signature reduction, the cloak put forth in [18] is the best option, and that this particular cloak satisfies Eqs. (10) and (11) and has a matched impedance at $r = b$. However, we have also noted the significant variation in the scattered field when different objects are placed in this cloak's hidden region. Is it possible to reduce this variation in the scattered field with different objects in the hidden region while maintaining the overall reduction in scattering width?

There are four parameters that must be met for a cylindrical cloak to be perfect: Eqs. (10),

(11), and (12) must be satisfied, and the cloak must have a matched impedance at $r = b$. To this point, we analyzed simplified cloaks that satisfy Eqs. (10) and (11), and that either do or do not have a matched impedance at $r = b$. We have found the cloak with the matched impedance results in the best improvement in scattering width even though this cloak has the largest field transmitted into its hidden region.

Now, consider a cloak with material parameters shown in Eq. (19).

$$\mu_r = 0.5, \quad \mu_\theta = \frac{r}{r-a}, \quad \epsilon_z = \frac{r-a}{r} \left(\frac{b}{b-a} \right)^2 \quad (19)$$

Like the improved parameter set put forth in [18], these parameters satisfy three of the four requirements. The difference is these parameters satisfy Eqs. (10) and (12) while having a matched impedance at $r = b$; Eq. (11) is not satisfied.

As we have done previously, we simulated a cloak having the constitutive parameters shown in Eq. (19) with a PEC cylinder of radius a and a square PEC of side length a in the hidden region. Note how the scattered fields for all three images shown in Fig. 13 appear very similar.

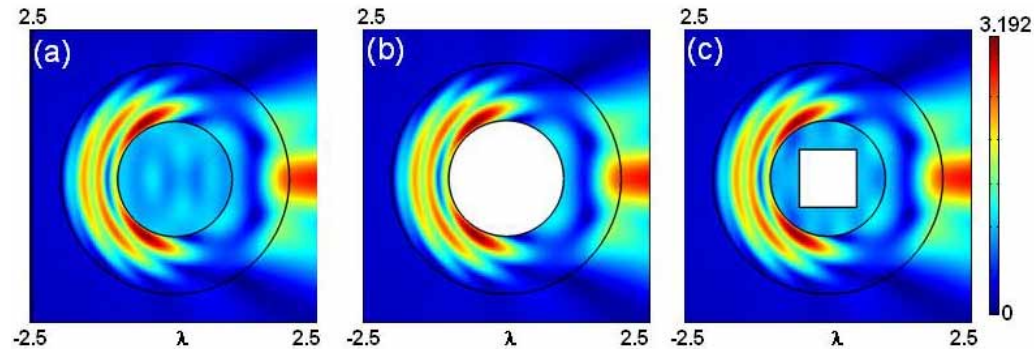


Fig. 13. Scattered electric field magnitude for a cylindrical cloak with parameters shown in Eq. (19) that has (a) nothing in its hidden region, (b) PEC cylinder with radius a in the hidden region, and (c) square PEC of side length a in the hidden region.

This suggests different objects in the hidden region have little effect on the scattered field. This can be seen more clearly by transforming the scattered fields to the far zone. This is shown in Fig. 14. The graphs in Fig. 14 clearly show there is no difference in the scattering width when different objects are placed in the hidden region of the cloak with parameters put forth in Eq. (19). Note the cyan and black lines lie virtually on top of the other. In fact, the average difference in the scattering widths is 0.0671 dB. This is because the total field in the hidden region is negligible. The field in the hidden region is negligible because the impedance at $r = a \rightarrow \infty$, which means no energy will be transmitted. Additionally, Fig. 14 shows scattering width results for a cloak using the parameters shown in Eq. (15). This is done to compare the performance of the cloaks in terms of scattering width. Obviously, the red and green lines are more desirable results because of the smaller scattering width values. However, this cloak's scattering widths vary more as a function of different objects in its hidden region. If various objects are going to be hidden and observation angles are in the specular region, the top cloak may be a better option. Of course, the cloak with parameters put forth in Eq. (19) has two radially varying parameters, meaning it is currently more difficult to manufacture.

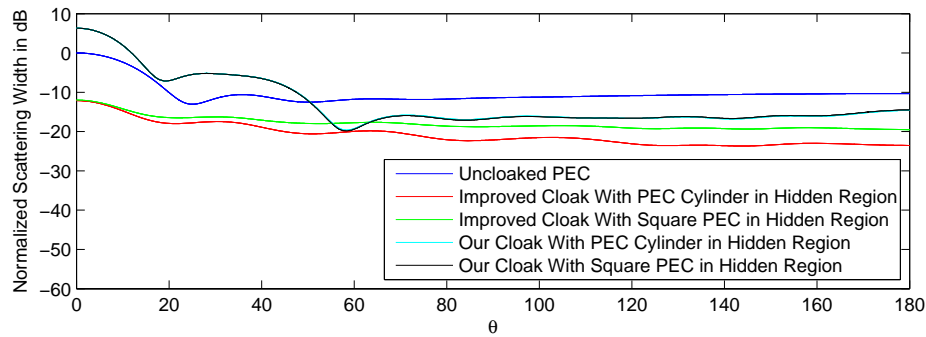


Fig. 14. Normalized scattering width from cloaks. The blue line is the scattering width for an uncloaked PEC, the red and green lines are the scattering widths for the improved cloak with parameters put forth in [18] and shown in Eq. (15) with a PEC cylinder and square PEC in the hidden region. The cyan and black lines are the same but for a cloak with material parameters shown in Eq. (19).

4. Conclusion

In this paper, we have analyzed the performance of simplified cylindrical cloaks with various constitutive parameters in order to understand the impact constitutive values have on field behavior. To date, the material parameters of simplified cloaks have focused on satisfying specific values of $\epsilon_z \mu_\theta$ and $\epsilon_z \mu_r$ while matching the impedance at the cloak's outer boundary. We have introduced a third constraint equation which helps control the overall effectiveness of the cylindrical cloak.

We analyzed cylindrical cloaks that satisfied the specific values for $\epsilon_z \mu_\theta$ and $\epsilon_z \mu_r$. We found that deviations from this third constraint equation resulted in larger fields being transmitted into a cylindrical cloak's hidden region. As the cloak's constitutive parameters were changed such that this new constraint was better satisfied, the amount of energy transmitted into the hidden region was shown to be reduced. However, the resulting impedance mismatch at $r = b$ due to changing the constitutive parameters resulted in a significant scattered field. However, despite reducing energy transmitted into the hidden region, which resulted in a reduction in the scattered field by the cloaked object, the cloak itself was creating a large scattered field. Hence, in terms of overall scattering width, having a matched impedance at $r = b$ seems to be more important than reducing the transmitted energy into the hidden region.

We then analyzed a particular cylindrical cloak that satisfied the specific values for $\epsilon_z \mu_\theta$ and μ'_θ while having a matched impedance at $r = b$. For observation angles in the backscatter region, we found this cloak to perform quite well in terms of scattering width as the scattered field was independent of objects placed in the hidden region. While scattering width performance was not on the same level as the cloak with parameters put forth in [18], the independence of the scattered field due to different objects in the hidden region is noteworthy.